

Journal of Materials Chemistry B

Accepted Manuscript



This is an *Accepted Manuscript*, which has been through the Royal Society of Chemistry peer review process and has been accepted for publication.

Accepted Manuscripts are published online shortly after acceptance, before technical editing, formatting and proof reading. Using this free service, authors can make their results available to the community, in citable form, before we publish the edited article. We will replace this *Accepted Manuscript* with the edited and formatted *Advance Article* as soon as it is available.

You can find more information about *Accepted Manuscripts* in the [Information for Authors](#).

Please note that technical editing may introduce minor changes to the text and/or graphics, which may alter content. The journal's standard [Terms & Conditions](#) and the [Ethical guidelines](#) still apply. In no event shall the Royal Society of Chemistry be held responsible for any errors or omissions in this *Accepted Manuscript* or any consequences arising from the use of any information it contains.

Renal Excreted Au clusters-EGFR antibody for targeted cancer radiation therapy

Xiao-Dong Zhang^a, Jie Chen^a, Jiang Yang^b, Jun-Ying Wang^a, Xiu Shen^a, Sha-Sha Song^a, Hao Wang^a, Hua He^c, Xiaojuan Wang^c, Saijun Fan^a, Yuan-Ming Sun^a, Meili Guo^d

Ultrasmall gold clusters have shown great potentials in biomedical applications. It is crucial to prepare targeting clusters with fast excretion properties. Here, we prepared gold cluster-EGFR antibody conjugates with cancer-specific targeting, enhanced therapeutic radiation and renal clearance properties, and then systematically investigated its targeted radiation therapy, clearance, and toxicity over a relatively long period of 25 days in mice. It was found that the as-prepared gold cluster-EGFR antibody conjugates showed higher *in vitro* uptakes than gold clusters alone in treated Hela cells and thus triggered more significant cancer radiation therapies than the nonspecific gold clusters. *In vivo* therapies and tumor uptakes showed that gold cluster-EGFR antibody conjugates could result in higher tumor uptakes and tumor ablations. Notably, gold cluster-EGFR antibody conjugates showed a urine excretion of 43% after 24 hours, only slightly lower than pure gold clusters (52%). Furthermore, hematological and biochemical studies showed that the conjugates did not cause liver and kidney toxicities after 30 days post injection. The present work showed that the targeting gold cluster-EGFR antibody conjugates with highly efficient therapeutic radiation, low toxicities and good excretions can be promising for medical applications.

Introduction

Gold nanomaterials have attracted extensive attentions in medical applications, such as drug deliveries, bioimaging, and cancer photothermal or radiation therapies.¹⁻⁷ However, the exogenous nanoparticles (NPs) which are large in size cannot escape from the reticulo-endothelial system (RES) absorption and thus lead to low uptakes in tumor, but high uptakes in liver and spleen.⁸⁻¹² It was reported that NPs with sizes >50 nm almost could not escape from RES absorption and caused appreciable liver distributions.¹³⁻¹⁷ In contrast, Au NPs with sizes <20 nm could reduce the RES absorption and induce certain tumor uptakes.¹⁸ Typical 20 nm PEG-protected Au NPs could present 6.63 % ID/g tumor uptakes, while 15 nm tiopronin-protected Au NPs showed 2.8 % ID/g tumor uptakes.^{19, 20} All these NPs can improve tumor uptakes through their long blood circulation time.^{21, 22} Unfortunately, these NPs with relatively large sizes still exhibited low tumour uptakes and cannot cross the 5.5 nm renal clearance barrier, causing potential liver toxicities.²³⁻²⁷

Gold clusters have attracted broad interests due to their unique structures, strong fluorescence, high tumour uptakes and highly efficient renal clearances.²⁶⁻³⁹ It was found that glutathione (GSH)-protected gold clusters exhibited high efficiencies and great potentials in cancer radiation therapies.^{29, 30, 40} Thus, it is desirable to conjugate targeting functional molecules to gold clusters to achieve active targeting therapies. The epidermal growth factor receptor (EGFR) antibody has been conceived as a highly efficient targeting molecule for cancer therapies and imaging. It was reported that the tumor uptake of EGFR antibody-Au NPs treated mice was much higher than untargeted Au NPs.⁴¹ Besides, in another important

application, EGFR antibody-Au NPs showed extremely efficient photothermal therapies and high tumor specificities.⁴² It also works effectively when carbon nanotubes were used as core materials for *in vivo* and *in vitro* drug deliveries.⁴³ Unfortunately, however, all those conjugates mentioned above cannot be well excreted. The hydrodynamic sizes of readily-available NP-EGFR antibody conjugates are so large that they cannot pass the renal filter.^{25, 28} Ultrasmall gold clusters with a hydrodynamic size of 2.8 nm can help improve the excretion.⁴⁴ In this study, we prepared a multifunctional gold cluster-EGFR antibody conjugate and achieved highly effective tumor uptakes and cancer radiation therapies as well as substantially efficient renal clearances.

Experimental Section

Materials and synthesis: The Au₂₉₋₄₃(GSH)₂₇₋₃₇ clusters were synthesized using a method reported previously.⁴⁴ Briefly, freshly-prepared aqueous solutions of HAuCl₄ (20 mM, 0.50 mL) and GSH (100 mM, 0.15 mL) were mixed with 4.35 mL of ultrapure water at 25 °C. The reaction mixture was heated to 70 °C under stirring (500 rpm) for 24 h. The resultant solution of gold clusters is light yellow in color under room light and shows strong orange emissions. The gold clusters were purified using ultrafiltration [with molecular weight cut-off (MWCO) of 3 kDa]. The raw products and purified solutions of gold clusters could be stored stably at 4 °C for 6 months with negligible changes in their optical properties.

Gold cluster-EGFR conjugation: The Au₂₉₋₄₃(GSH)₂₇₋₃₇ clusters (3 mM Au concentration) were mixed with *N*-Hydroxysuccinimide (50 mg) and ethyl (dimethylaminopropyl) carbodiimide (50 mg) and

then washed 3 times to remove unreacted NHS and EDC using Amicon 30k filter devices in water. Afterwards, EGFR monoclonal antibodies (20 μM) were added to activate gold clusters and the reaction was allowed to stand for 2 hours. After reaction, the samples were purified using ultrafiltration [with molecular weight cut off (MWCO) of 100kDa] to remove any free gold clusters. Finally, the Amicon 300k filter devices were used to remove complexes of large particles.

Materials characterization: Transmission electron microscopy (TEM) analysis was conducted with a JEOL JEM-2100F microscope operated at 200kV. The zeta-potential analysis and hydrodynamic size of the gold clusters were determined by the Nano-ZS Zetasizer particle analyzer (Malvern). Data were acquired in the phase analysis light scattering mode at 25°C and sample solutions were prepared by diluting gold clusters into 10 mM PBS solution (pH 7.0). The UV-vis absorption spectra were recorded on a UV-1800 spectrophotometer (Shimadzu). The photoluminescence (PL) spectra were measured by a fluorescence spectrophotometer (F4600, Hitachi) under an excitation of 370 nm. Stability of gold clusters was evaluated from fluorescence spectra.

In vitro cytotoxicity test: HeLa cells were cultured at 37 °C under humidified atmosphere with 5% CO₂ and high-glucose Dulbecco's modified Eagle's medium (DMEM) which contained fetal calf serum (10%), L-glutamine (2.9 mg/mL), streptomycin (1 mg/mL), and penicillin (1000 units/mL). The cells (in culture medium) were dispensed in 96-well plates (90 μL containing 6000 cells per well). Gold clusters and gold cluster-EGFR antibodies (10 μL) were then added to each well at different concentrations. The effect of different concentrations of gold clusters and gold cluster-EGFR antibodies was assessed using MTT Cell Proliferation and Cytotoxicity Assay Kit. After 24 and 48 hours of treatments, 10 μL of MTT reagent was added and the incubation stayed for 4 hours. The media were then replaced with 150 μL DMSO. The optical absorption at 490 nm was recorded with a single tube luminometer (TD 20/20, Turner Biosystems Inc., Sunnyvale, CA, USA). Meanwhile, the fluorescence was recorded by fluorescence spectrophotometer (F4600, Hitachi) for cellular uptakes.

In vitro radiation therapy: HeLa cells were incubated in 96-well plates (6000 per well) overnight and exposed to gold clusters or gold cluster-EGFR antibodies (100 μL , 200 $\mu\text{g}/\text{mL}$) for another 24 hours. The cells were then irradiated under gamma rays from ¹³⁷Cs (photon energy 662 keV) with an activity of 3600 Ci at doses of 1, 2, 4, 6, and 8 Gy. After 24 hours of irradiation, cell viabilities were measured by MTT assays.

Animal injection and sample collection: Animals were purchased, maintained, and handled with protocols approved by the Institute of Radiation Medicine, Chinese Academy of Medical Sciences (IRM, CAMS). BALB/c mice at 11 weeks of age were obtained from IRM laboratories and housed by 2 mice per cage at a 12 h/12 h light/dark cycle with food and water supplied. Forty-eight mice were divided into six groups with eight mice per group. The U14 tumor models were generated by subcutaneous injections of 2×10^6 cells in 50 μL of PBS into the right shoulders of male mice. The mice were treated with gold clusters and EGFR antibody-gold clusters (3 mM). The main organs, such as tumor, liver, kidney, spleen, heart, lung and brain were collected.

Hematology, biochemistry, and pathology: Using a standard saphenous vein blood collection technique, blood was drawn for hematology analysis (potassium EDTA collection tube). The analysis of standard hematological and biochemical examinations was performed. For blood analysis, 1 mL of blood was collected from mice and separated by centrifugation into cellular and plasma fractions. Mice were sacrificed by isoflurane anesthetic gas and major organs from those mice were harvested, fixed in 10% neutral

buffered formalin, processed routinely into paraffin and stained by hematoxylin and eosin staining (H&E staining). Pathologies were examined by a digital microscope.

Biodistribution: The organs and original solutions from the gold cluster- and EGFR antibody-gold cluster-treated mice (3 samples per group) were digested using a microwave system CEM Mars 5 (CEM, Kamp Lintfort, Germany). The Au concentration was measured with an ICP-MS (Agilent7500 CE, Agilent Technologies, Waldbronn, Germany).

Statistical analyses: All data presented herein were shown as the average \pm SD from experiments repeated three times or more. The paired Student's t-test was used for statistical analysis.

Results and Discussion

Physical properties of luminescent GSH-Au clusters are presented in Fig.1. A representative transmission electron microscopy (TEM) image (**Figure 1a**) showed that the GSH-Au clusters have a size below 2 nm. The hydrodynamic size of gold clusters is measured to be 2.8 nm (**Figure 1b**). After EGFR antibody conjugation, only insignificant changes were found in optical absorption spectra (**Figure 1c**). In addition, the as-prepared gold clusters and EGFR antibody-gold clusters both showed orange emissions with the emission peaks at ~ 610 nm using excitation wavelength of 370 nm (**Figure 1d**). The EGFR antibody-gold cluster conjugates also showed a good stability in solution. No obvious changes in luminescence intensities were observed even after 90 days of storage at 4 °C, which is in good agreement with available data.⁴⁵ The Au clusters behave as a supramolecular structure with small molecular ligands and present the ultrasmall hydrodynamic size, consistent with previous work.^{27, 30} Besides, larger EGFR antibody-gold cluster aggregates were removed using 300 k filter, so the size of collected EGFR antibody-gold cluster conjugates is therefore guaranteed to be ultrasmall.

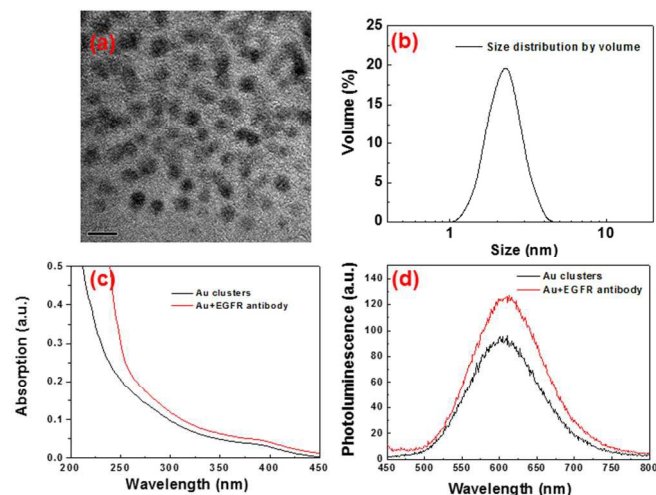


Figure 1. (a) TEM image and (b) hydrodynamic size using dynamic light scattering of gold clusters, (c) absorption, and (d) photoemission of gold clusters and EGFR antibody-gold clusters. Scale bar=5 nm.

Cellular responses (or cytotoxicity) of the gold clusters and EGFR antibody-gold clusters were investigated using HeLa cells. The HeLa cells were treated with gold clusters and EGFR antibody-gold clusters at different concentrations from 0.3 nM to 3 mM. As shown in **Figure 2a** and **2b**, the viabilities of cells change very little after 24 hours and 48 hours as the concentrations of gold clusters and EGFR antibody-gold clusters increase, which indicates a low cytotoxicity

even at such a high concentration as 3 mM. Indeed, the EGFR antibody and gold clusters show good cytotoxicity by themselves, so it is as expected that gold cluster-EGFR antibody conjugates do not show apparent cytotoxicities in the concentrations investigated, which is consistent with previous results.^{46,47} Next we performed the cellular uptakes of gold clusters and EGFR antibody-gold cluster conjugates using fluorescence approaches. It is found that cells treated with gold clusters show increasing cellular uptakes with increasing cluster concentrations and the uptake is up to 28 % after 24 hour incubations (**Figure 2c**). In contrast, the targeting EGFR antibody-gold clusters show a similar trend and the cellular uptake increases to 45%, indicating higher uptakes. It is clear that the targeting conjugation can induce more significant and specific cellular uptakes. In the previous work, it has been reported that EGFR antibody-coated NPs could induce 67% internalization while cellular uptakes are only 10% for nonspecific NPs.⁴⁸ The cellular uptake of gold clusters is higher than that of large gold NPs due to their ultrasmall sizes and conjugated targeting molecules.⁴⁹ It has been found that particles in nanoscale could perform higher cellular uptakes than that of microscaled particles.⁴⁹ Besides, the cellular uptakes and localizations of NPs are closely related to cell lines and surface charges of NPs.⁵⁰⁻⁵² GSH can minimize protein adsorption in physiological environments which are also helpful for cellular uptakes.⁵² We then carried out the radiation therapies. The *in vitro* radiation enhancements of the gold clusters and EGFR antibody-gold clusters were measured by MTT assays using HeLa cells. As shown in **Figure 2d**, an obviously increasing radiation along with increasing dosages can be observed for the cell cultures treated with gold clusters and EGFR antibody-gold clusters. Cells treated with EGFR antibody-gold clusters manifest a more significant radiation therapy than those treated with nonspecific gold clusters. The radiation enhancement could be caused by the increased DNA damages from the photoelectric effect and Compton scattering of the heavy metal (Au).^{47,53} As a result, the EGFR antibody-gold cluster conjugates can both increase cellular uptakes and efficiently induce radiation enhancements.

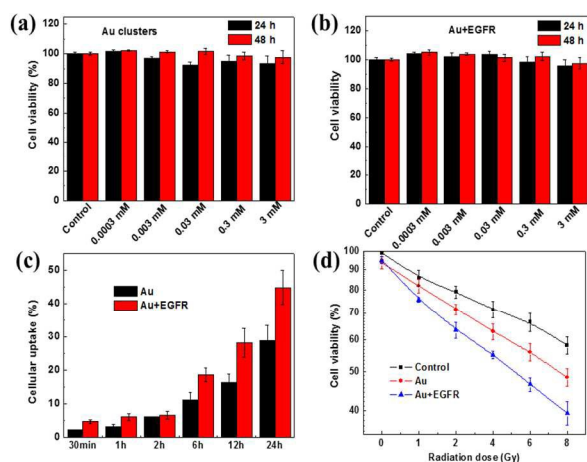


Figure 2. Viability of HeLa cells after incubation with the (a) gold clusters and (b) EGFR-gold clusters for 24 and 48 hours. (c) Cellular uptake of gold clusters and EGFR-gold clusters after different incubation time. (d) Viability of HeLa cells treated with only radiation [control, black line], the gold clusters + radiation [red line], and the EGFR antibody-gold clusters + radiation [blue line].

Encouraged by the highly effective cellular uptakes and *in vitro* experiments of Au clusters and EGFR antibody-gold clusters in tumor cells, *in vivo* cancer radiation therapy was carried out using

U14 tumor-bearing BALB/c mice. The gold clusters and EGFR antibody-gold cluster conjugates were intraperitoneally injected into mice (3mM, 200 μ L). After 2 hours, the mice were locally irradiated under ¹³⁷Cs gamma radiation of 3600 Ci at the dose of 5 Gy. The volume of the tumor was monitored by the Student's T-test (**Figure 3a**). Without the radiation treatment, the tumor volume at the beginning steadily increases by 3.8 times after 25 days, regardless of the existence of the gold clusters or EGFR antibody-gold clusters. With the radiation treatment, the growth of the tumor volume in mice without nanocluster injection (radiation only) is retarded by 7 days, but the tumor eventually grows to 2.5 times after 25 days. The tumor volume of the gold cluster-treated mice under radiation is 1.51 times after 25 days, which is a significant reduction in the growth rate. In contrast, the tumor volume of the EGFR antibody-gold cluster-treated mice under radiation is only 0.89 times after 25 days, demonstrating a much smaller tumor in volume. Moreover, we sacrificed all mice, collected all tumor tissues after 25 days of treatments and evaluated the tumor weights of controls and treated mice. The tumor weight of mice treated with EGFR antibody-gold clusters and radiation exhibited a tumor weight of only 0.15 g, which is much less than that of gold cluster-treated mice (0.25 g) or the only radiation-treated controls (0.48 g) (**Figure 3b**). These *in vivo* results prove that the EGFR antibody-gold clusters have a good targeting capability and strong radiation-enhancing effects. EGFR antibody-conjugated nanomaterials have also been shown to induce high tumor uptakes in photothermal imaging and biodetections.^{41,42} Similarly, the effects of cancer radiation therapies based on heavy metal elements mainly depend on their concentrations in tumor and the photoelectric absorptions. The effective targeting in tumor tissue and the unique X-ray absorption induce obvious inhibition of tumor growth under radiation. Besides, 662 keV high energy gamma photons also assure high penetrability and lots of photons can reach deep into tumor tissues to achieve desired therapies.

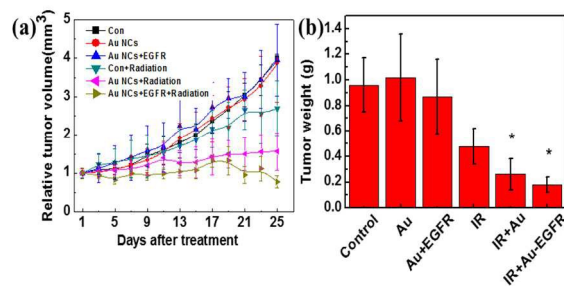


Figure 3. Time-course studies of tumor (a) volume and (b) weight of mice treated with gold clusters and EGFR-gold clusters.

To reveal the *in vivo* targeting capabilities of EGFR antibody-gold clusters, we investigated the biodistribution and renal excretion of gold clusters and EGFR antibody-gold clusters. Mice were sacrificed on day 25 after radiation therapies. Au amount in major organs (3 mice per group) was determined by inductively coupled plasma mass spectrometry (ICP-MS). The biodistribution data were presented as in **Figure 4a**. The testes, kidney, liver, and spleen were the dominant organs for uptakes of gold clusters. Lung and brain showed relatively low Au contents, similar to the previous findings.^{27,28} It is surprising that the EGFR antibody-gold clusters showed a significant 4-time higher tumor uptake than that of the gold cluster-treated mice. It is clear that the EGFR antibody-gold clusters can cause significant tumor uptakes by their active targeting abilities, corresponding well to the results of radiation therapies. Besides, it is clear that Au contents in gold cluster- and EGFR antibody-gold cluster-treated

mice are similar, indicating good excretions of gold clusters even after conjugation of EGFR antibodies. As such, we further confirmed their renal excretion in mice treated with gold clusters and EGFR antibody-gold clusters using ICP-MS. **Figure 4b** showed the time-dependent accumulated renal excretions of gold clusters and EGFR antibody-gold clusters. Briefly, the gold clusters and EGFR antibody-gold clusters of 200 μL 3 mM were intraperitoneally injected into mice and the urine was collected at different time points. It is obvious that gold clusters show faster excretions with time and about 52 % gold clusters could be excreted after 24 hours, consistent with previous extensive investigations. In the meantime, the EGFR antibody-gold clusters also show good excretions and the accumulated renal excretion is up to 43% after 24 hours, which is very close to available data on renal clearances.²⁶ Thus it is suggested that EGFR antibody-gold clusters still maintain the capability of highly efficient renal clearances even after conjugation. At present, small gold clusters can show good renal excretions, but can hardly achieve active targeting, which hinders their tumor uptakes and cancer radiation therapies. Thus, it is an unmet need to prepare gold clusters with both highly specific targeting abilities and effective renal clearances. The present work provides such potentials with actively targeting gold clusters with minimized toxicities.

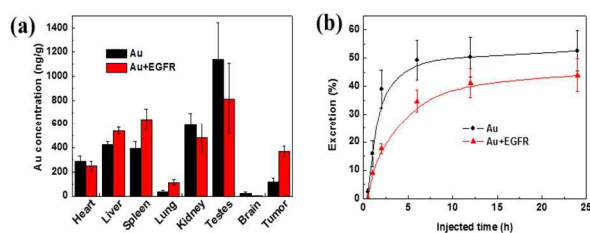


Figure 4. (a) Biodistribution of mice treated with gold clusters and EGFR-gold clusters, and (b) accumulated time-dependent Au concentration in urine of the mice treated with gold clusters and EGFR-gold clusters.

To address the *in vivo* toxicities, we used the gold-standard clinical biochemical markers for the toxicity analyses of injected gold clusters and EGFR antibody-gold clusters in mice, including alanine aminotransferase (ALT), aspartate aminotransferase (AST), albumin (ALB), blood urea nitrogen (BUN), creatinine (CREA) and globulin (GLOB). 200 μL 3 mM solutions of gold clusters and EGFR antibody-gold clusters were intraperitoneally injected into mice and all biochemical indicators were collected after 25 days. The hematology data are presented in **Figure 5**, where no obvious differences in the two common indicators (ALT and AST) could be observed in mice treated with gold clusters and EGFR antibody-gold clusters, as compared to those untreated. The as-prepared gold clusters and EGFR antibody-gold clusters do not induce any potential toxicological responses. Moreover, we also examined the standard biochemical and pathological changes of heart, liver, spleen, and kidney by immunohistochemistry. No significant losses of the body weight (Figure S1a) or abnormal organ indices (Figure S1b–c) were observed. Pathological changes were then evaluated. As shown in **Figure 6**, no obvious organ damages could be observed in liver, spleen, and kidney in the period of 25 days post injection with gold clusters and EGFR antibody-gold clusters.

Previous studies demonstrated that the potential toxicities of functional nanomaterials are mostly correlated to their clearances in the body.^{27, 54} However, the actual *in vivo* pharmacokinetics of functional nanomaterials could be even more complicated. The data presented in this study clearly indicated that the EGFR antibody-

gold clusters could be efficiently cleared by kidney. Therefore, the present work suggests the EGFR antibody-gold clusters are promising for active targeting therapies and imaging for further medical applications. It also has potentials as cancer radiation therapies of gold cluster-based complexes. Smaller peptides as targeting molecules for conjugations with gold clusters are still promising to be developed for medical applications. The quantum yield of gold clusters is still not sufficiently high and it is necessary to be improved for potential bioimaging in the future. Besides, it is important to clarify radiation energy-dependent cancer radiation therapies, which will be valuable for further clinical applications.

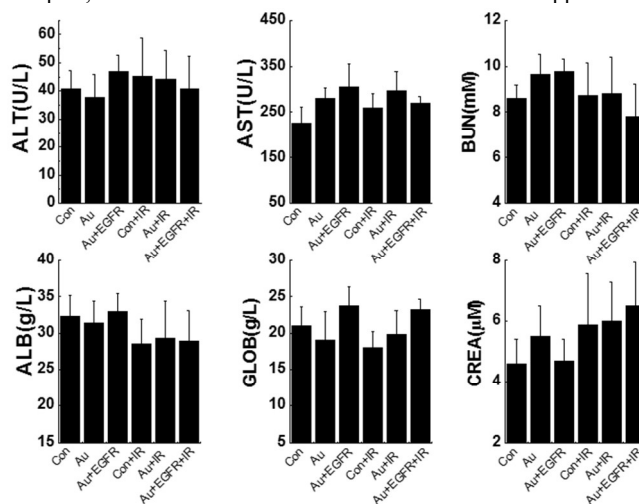


Figure 5. Blood biochemical analysis of mice treated with the gold clusters and EGFR-gold clusters. The results showed the mean and standard deviation of alanine aminotransferase (ALT), aspartate aminotransferase (AST), albumin (ALB), bloodurea nitrogen (BUN), creatinine (CREA), and globulin (GLOB).

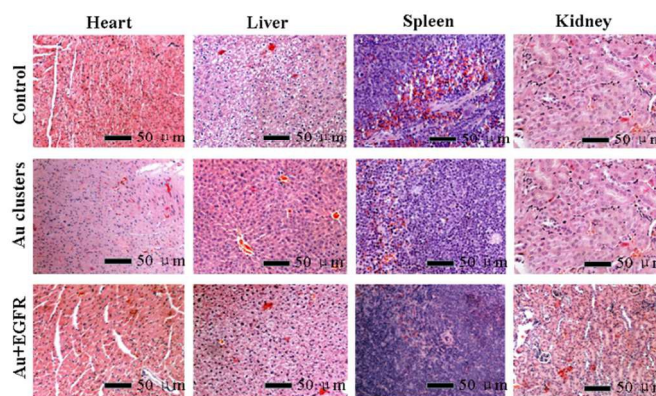


Figure 6. Pathological data from the heart, liver, spleen, and kidney of mice treated with gold clusters and EGFR-gold clusters. Scale bars, 50 μm .

Conclusion

In summary, we prepared a multifunctional EGFR antibody-gold cluster conjugates with targeting ability, low toxicities and renal cleared properties and investigated their biological responses in detail. It is found that EGFR antibody-gold clusters could increase the cellular uptakes and cancer radiation therapies *in vitro* compared with nonspecific gold clusters. Furthermore, it is found that EGFR antibody-gold clusters show a significantly higher tumor uptake and a more significant tumor ablation than the non-targeting gold

clusters. Finally, we found that EGFR antibody-gold clusters could still be rapidly excreted by kidney without any toxic responses. The current work clearly shows that the EGFR antibody-gold clusters are interesting in further medical applications in the future.

ACKNOWLEDGMENT

This work was supported by the National Natural Science Foundation of China (Grant No.81471786 and 11304220), Natural Science Foundation of Tianjin (Grant No. 13JCQNJC13500) and Foundation of Union New Star, CAMS (N4o.1256).

Note

^aTianjin Key Laboratory of Molecular Nuclear Medicine, Institute of Radiation Medicine, Chinese Academy of Medical Sciences and Peking Union Medical College, No. 238, Baidi Road, Tianjin 300192, China.

Email: xiaodongzhang@tju.edu.cn

Email: sunyuanming@irm-cams.ac.cn

^bDepartment of Biological Systems Engineering, University of Wisconsin-Madison, Madison, WI, USA

^cCentre for Bioengineering and Biotechnology, China University of Petroleum (East China), 66 Changjiang West Road, Qingdao 266555, China.

^dDepartment of Physics, School of Science, Tianjin Chengjian University, No. 26, Jinjing Road, Tianjin 300384, China

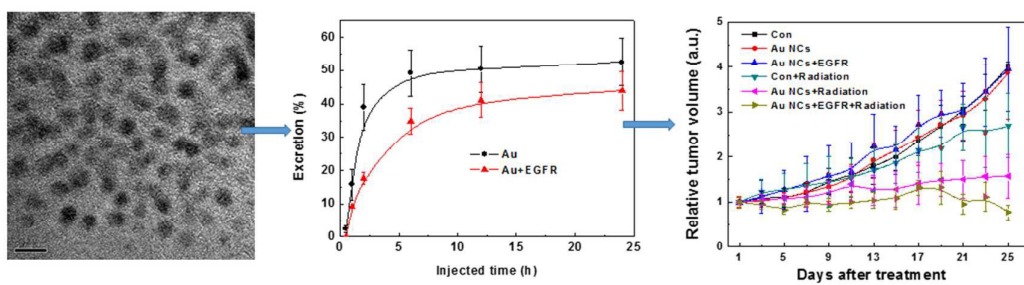
Email: guomeili@tjuci.edu.cn

REFERENCES

- X. Huang, I. H. El-Sayed, W. Qian and M. A. El-Sayed, *J. Am. Chem. Soc.*, 2006, **128**, 2115-2120.
- J. Chen, F. Saeki, B. J. Wiley, H. Cang, M. J. Cobb, Z.-Y. Li, L. Au, H. Zhang, M. B. Kimmey and X. Li, *Nano Lett.*, 2005, **5**, 473-477.
- A. Javey and H. Dai, *J. Am. Chem. Soc.*, 2005, **127**, 11942-11943.
- N. L. Rosi, D. A. Giljohann, C. S. Thaxton, A. K. Lytton-Jean, M. S. Han and C. A. Mirkin, *Science*, 2006, **312**, 1027-1030.
- J. Yang, S. Deng, J. Lei, H. Ju and S. Gunasekaran, *Biosens. Bioelectron.*, 2011, **29**, 159-166.
- X.-D. Zhang, D. Wu, X. Shen, J. Chen, Y.-M. Sun, P.-X. Liu and X.-J. Liang, *Biomaterials*, 2012, **33**, 6408-6419.
- P. Huang, J. Lin, S. Wang, Z. Zhou, Z. Li, Z. Wang, C. Zhang, X. Yue, G. Niu and M. Yang, *Biomaterials*, 2013, **34**, 4643-4654.
- C. H. J. Choi, J. E. Zuckerman, P. Webster and M. E. Davis, *Proc. Natl. Acad. Sci. USA*, 2011, **108**, 6656-6661.
- J. Lipka, M. Semmler-Behnke, R. A. Sperling, A. Wenk, S. Takenaka, C. Schleh, T. Kissel, W. J. Parak and W. G. Kreyling, *Biomaterials*, 2010, **31**, 6574-6581.
- S. K. Balasubramanian, J. Jittiwat, J. Manikandan, C.-N. Ong, E. Y. Liya and W.-Y. Ong, *Biomaterials*, 2010, **31**, 2034-2042.
- W. H. De Jong, W. I. Hagens, P. Krystek, M. C. Burger, A. J. Sips and R. E. Geertsma, *Biomaterials*, 2008, **29**, 1912-1919.
- X.-D. Zhang, D. Wu, X. Shen, P.-X. Liu, N. Yang, B. Zhao, H. Zhang, Y.-M. Sun, L.-A. Zhang and F.-Y. Fan, *Int. J. Nanomed.*, 2011, **6**, 2071-2081.
- G. Sonavane, K. Tomoda and K. Makino, *Colloids Surf. B.*, 2008, **66**, 274-280.
- M. Janát-Amsbury, A. Ray, C. Peterson and H. Ghandehari, *Eur. J. Pharm. Biopharm.*, 2011, **77**, 417-423.
- X. D. Zhang, J. Chen, Y. Min, G. B. Park, X. Shen, S. S. Song, Y. M. Sun, H. Wang, W. Long and J. Xie, *Adv. Funct. Mater.*, 2014, **24**, 1718-1729.
- S. Sun, B. Y. Xia, J. Chen, J. Yang, X. Shen, S. Fan, M. Guo, Y. Sun and X. Zhang, *RSC Adv.*, 2014, **4**, 42598-42603.
- G. Hong, Y. Zou, A. L. Antaris, S. Diao, D. Wu, K. Cheng, X. Zhang, C. Chen, B. Liu and Y. He, *Nature Comm.*, 2014, **5**, 5206.
- L. Balogh, S. S. Nigavekar, B. M. Nair, W. Lesniak, C. Zhang, L. Y. Sung, M. S. Kariapper, A. El-Jawahri, M. Llanes and B. Bolton, *Nanomed-Nanotechnol.*, 2007, **3**, 281-296.
- G. von Maltzahn, J.-H. Park, A. Agrawal, N. K. Bandaru, S. K. Das, M. J. Sailor and S. N. Bhatia, *Cancer Res.*, 2009, **69**, 3892-3900.
- K. Huang, H. Ma, J. Liu, S. Huo, A. Kumar, T. Wei, X. Zhang, S. Jin, Y. Gan and P. C. Wang, *ACS Nano*, 2012, **6**, 4483-4493.
- J. T. Robinson, G. Hong, Y. Liang, B. Zhang, O. K. Yaghi and H. Dai, *J. Am. Chem. Soc.*, 2012, **134**, 10664-10669.
- A. Al Zaki, D. Joh, Z. Cheng, A. L. B. De Barros, G. Kao, J. Dorsey and A. Tsourkas, *ACS Nano*, 2014, **8**, 104-112.
- X.-D. Zhang, H.-Y. Wu, D. Wu, Y.-Y. Wang, J.-H. Chang, Z.-B. Zhai, A.-M. Meng, P.-X. Liu, L.-A. Zhang and F.-Y. Fan, *Int. J. Nanomed.*, 2010, **5**, 771-781.
- J. Chen, H. Wang, W. Long, X. Shen, D. Wu, S.-S. Song, Y.-M. Sun, P.-X. Liu, S. Fan and F. Fan, *Int. J. Nanomed.*, 2013, **8**, 2409-2419.
- H. S. Choi, W. Liu, P. Misra, E. Tanaka, J. P. Zimmer, B. I. Ipe, M. G. Bawendi and J. V. Frangioni, *Nat. Biotechnol.*, 2007, **25**, 1165-1170.
- C. Zhou, M. Long, Y. Qin, X. Sun and J. Zheng, *Angew. Chem. Int. Ed.*, 2011, **123**, 3226-3230.
- X.-D. Zhang, D. Wu, X. Shen, P.-X. Liu, F.-Y. Fan and S.-J. Fan, *Biomaterials*, 2012, **33**, 4628-4638.
- X. D. Zhang, Z. Luo, J. Chen, H. Wang, S. S. Song, X. Shen, W. Long, Y. M. Sun, S. Fan and K. Zheng, *Small*, 2015, **11**, 1683-1690.
- J. Liu, M. Yu, C. Zhou, S. Yang, X. Ning and J. Zheng, *J. Am. Chem. Soc.*, 2013, **135**, 4978-4981.
- X. D. Zhang, Z. Luo, J. Chen, X. Shen, S. Song, Y. Sun, S. Fan, F. Fan, D. T. Leong and J. Xie, *Adv. Mater.*, 2014, **26**, 4565-4568.
- C. A. Simpson, K. J. Salleng, D. E. Cliffler and D. L. Feldheim, *Nanomed-Nanotechnol.*, 2013, **9**, 257-263.
- J. Xie, Y. Zheng and J. Y. Ying, *J. Am. Chem. Soc.*, 2009, **131**, 888-889.
- Y. Yu, Z. Luo, D. M. Chevrier, D. T. Leong, P. Zhang, D.-e. Jiang and J. Xie, *J. Am. Chem. Soc.*, 2014, **136**, 1246-1249.
- S. Wang, X. Meng, A. Das, T. Li, Y. Song, T. Cao, X. Zhu, M. Zhu and R. Jin, *Angew. Chem. Int. Ed.* 2014, **53**, 2376-2380.
- H. Chen, B. Li, X. Ren, S. Li, Y. Ma, S. Cui and Y. Gu, *Biomaterials*, 2012, **33**, 8461-8476.

36. Y. Wang, J. Chen and J. Irudayaraj, *ACSNano*, 2011, **5**, 9718-9725.
37. M. Zhu, C. M. Aikens, F. J. Hollander, G. C. Schatz and R. Jin, *J. Am. Chem. Soc.*, 2008, **130**, 5883-5885.
38. R. Jin, *Angew. Chem. Int. Ed.*, 2008, **47**, 6750-6753.
39. R. Jin, *Nanoscale*, 2010, **2**, 343-362.
40. X. D. Zhang, J. Chen, Z. Luo, D. Wu, X. Shen, S. S. Song, Y. M. Sun, P. X. Liu, J. Zhao and S. Huo, *Adv. Healthcare Mater.*, 2014, **3**, 133-141.
41. X. Qian, X.-H. Peng, D. O. Ansari, Q. Yin-Goen, G. Z. Chen, D. M. Shin, L. Yang, A. N. Young, M. D. Wang and S. Nie, *Nat. Biotechnol.*, 2008, **26**, 83-90.
42. I. H. El-Sayed, X. Huang and M. A. El-Sayed, *Cancer Lett.*, 2006, **239**, 129-135.
43. A. A. Bhirde, V. Patel, J. Gavard, G. Zhang, A. A. Sousa, A. Masedunskas, R. D. Leapman, R. Weigert, J. S. Gutkind and J. F. Rusling, *ACS Nano*, 2009, **3**, 307-316.
44. Z. Luo, X. Yuan, Y. Yu, Q. Zhang, D. T. Leong, J. Y. Lee and J. Xie, *J. Am. Chem. Soc.*, 2012, **134**, 16662-16670.
45. L. Shang, N. Azadfar, F. Stockmar, W. Send, V. Trouillet, M. Bruns, D. Gerthsen and G. U. Nienhaus, *Small*, 2011, **7**, 2614-2620.
46. Y. Qian, M. Qiu, Q. Wu, Y. Tian, Y. Zhang, N. Gu, S. Li, L. Xu and R. Yin, *Sci. Rep.*, 2014, **4**, 7490.
47. R. Popovtzer, A. Agrawal, N. A. Kotov, A. Popovtzer, J. Balter, T. E. Carey and R. Kopelman, *Nano Lett.*, 2008, **8**, 4593-4596.
48. F. M. Mickler, L. Möckl, N. Ruthardt, M. Ogris, E. Wagner and C. Bräuchle, *Nano Lett.*, 2012, **12**, 3417-3423.
49. C. Brandenberger, C. Mühlfeld, Z. Ali, A. G. Lenz, O. Schmid, W. J. Parak, P. Gehr and B. Rothen - Rutishauser, *Small*, 2010, **6**, 1669-1678.
50. C. Schleh, M. Semmler-Behnke, J. Lipka, A. Wenk, S. Hirn, M. Schäffler, G. Schmid, U. Simon and W. G. Kreyling, *Nanotoxicology*, 2012, **6**, 36-46.
51. C. D. Walkey, J. B. Olsen, H. Guo, A. Emili and W. C. Chan, *J. Am. Chem. Soc.*, 2012, **134**, 2139-2147.
52. R. D. Vinluan III, J. Liu, C. Zhou, M. Yu, S. Yang, A. Kumar, S. Sun, A. Dean, X. Sun and J. Zheng, *ACS Appl. Mater. Interfaces*, 2014, **6**, 11829-11833.
53. K. T. Butterworth, S. J. McMahon, F. J. Currell and K. M. Prise, *Nanoscale*, 2012, **4**, 4830-4838.
54. S. Fraga, A. Brandão, M. E. Soares, T. Morais, J. A. Duarte, L. Pereira, L. Soares, C. Neves, E. Pereira and M. de Lourdes Bastos, *Nanomed-Nanotechnol.*, 2014, **10**, 1757-1766.

A table of contents



EGFR antibody-Gold clusters can achieve the highly efficient radiation therapy and renal clearance